JACS
JOURNAL OF THE AMERICAN CHEMICAL SOCIETY

Article

pubs.acs.org/JACS

Cell-Permeable Cyclic Peptides from Synthetic Libraries Inspired by Natural Products

William M. Hewitt,[†] Siegfried S. F. Leung,[‡,⊥] Cameron R. Pye,[†] Alexandra R. Ponkey,[†] Maria Bednarek,[§] Matthew P. Jacobson,*[,‡] and R. Scott Lokey*[,†]

[†]Department of Chemistry and Biochemistry, University of California, Santa Cruz, California 95064, United States
[‡]Department of Pharmaceutical Chemistry, University of California, San Francisco, California 94143, United States
[§]Department of Antibody Discovery & Protein Engineering, Medimmune Ltd., Cambridge CB21 6GH, U.K.

Supporting Information

ABSTRACT: Drug design efforts are turning to a new generation of therapeutic targets, such as protein−protein interactions (PPIs), that had previously been considered "undruggable" by typical small molecules. There is an emerging view that accessing these targets will require molecules that are larger and more complex than typical small molecule drugs. Here, we present a methodology for the discovery of geometrically diverse, membrane permeable cyclic peptide scaffolds based on the synthesis and permeability screening of a combinatorial library, followed by deconvolution of membrane-permeable scaffolds to identify cyclic peptides with good to excellent passive cell permeabilities. We use a combination of experimental and computational approaches to investigate structure-permeability relationships in one of these scaffolds, and uncover structural and conformational factors that govern passive membrane diffusion in a related set of cyclic peptide diastereomers. Further, we investigate the dependency of permeability on side-chain identity of one of these scaffolds through single-point diversifications to show the adaptability of these scaffolds toward development of permeability-biased libraries suitable for bioactivity screens. Overall, our results demonstrate that many novel, cell permeable scaffolds exist beyond those found in extant natural products, and that such scaffolds can be rapidly identified using a combination of synthesis and deconvolution which can, in principle, be applied to any type of macrocyclic template.

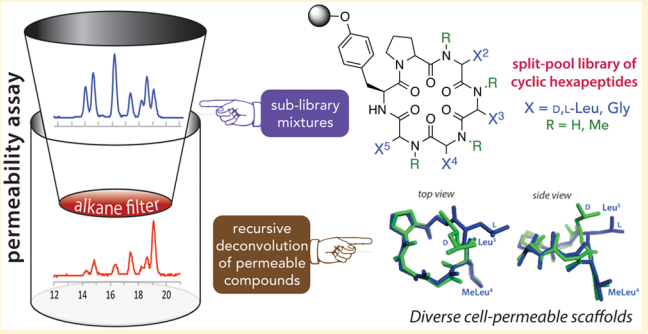

INTRODUCTION

Recent biomedical advances have produced a wave of candidate therapeutic targets, many of which are intracellular protein−DNA, protein−RNA, and protein−protein interactions (PPIs) whose binding interfaces are larger and less pocket-like than typical drug targets.[1,2] While many large binding sites are considered "undruggable" by small molecules, they can often be inhibited by larger, more complex molecules such as intracellularly expressed antibodies (intrabodies)[3−5] as well as natural and synthetic cyclic peptides.[6−11] Indeed, the prevalence of potent, PPI-disrupting cyclic peptides highlights the potential utility of these compounds as therapeutics.[12−14] However, this increased molecular weight (MW) and complexity comes at a cost, as larger, more functionally rich molecules often fail to meet the physicochemical requirements (captured by rough bioavailability predictors such as Lipinski's "Rule of 5")[15,16] for cell permeability, thus limiting them in most cases to parenteral delivery against extracellular targets.

Nonetheless, there is a class of compounds exemplified by the cyclic peptide cyclosporine A (CSA; MW 1202 Da) that exhibit drug-like cell permeability and, in some cases, oral bioavailability, despite molecular weights that lie well outside the range of typical small molecule drugs (i.e., ∼500−700 Da). While physical models of permeability for conventional drug-like molecules are well established,[17] the determinants of passive membrane diffusion in molecules at the larger end of the MW continuum are somewhat less well understood,[18] hindering the rational design of cell-permeable, "beyond-Rule-of-5" (bRo5) molecules as therapeutic agents. As interest grows in designing cyclic peptides and other macrocycles against intracellular targets,[19,20] understanding the relationship between structure and permeability in these bRo5 molecules will be vital.

Previously we reported model cyclic peptides[21−23] whose passive permeabilities, like CSA, depend on conformation-determining backbone elements such as stereochemistry and *N*-methylation.[24] Here, we describe the synthesis of an exhaustive library of 1152 cyclic hexapeptide stereoisomers and *N*-methyl variants—prepared and screened as 12 sub-libraries consisting of 96 cyclic peptides—inspired by the diverse backbone geometries found in cyclic peptide natural products (i.e.,

Received: September 2, 2014
Published: December 17, 2014

DOI: 10.1021/ja508766b
J. Am. Chem. Soc. 2015, 137, 715−721

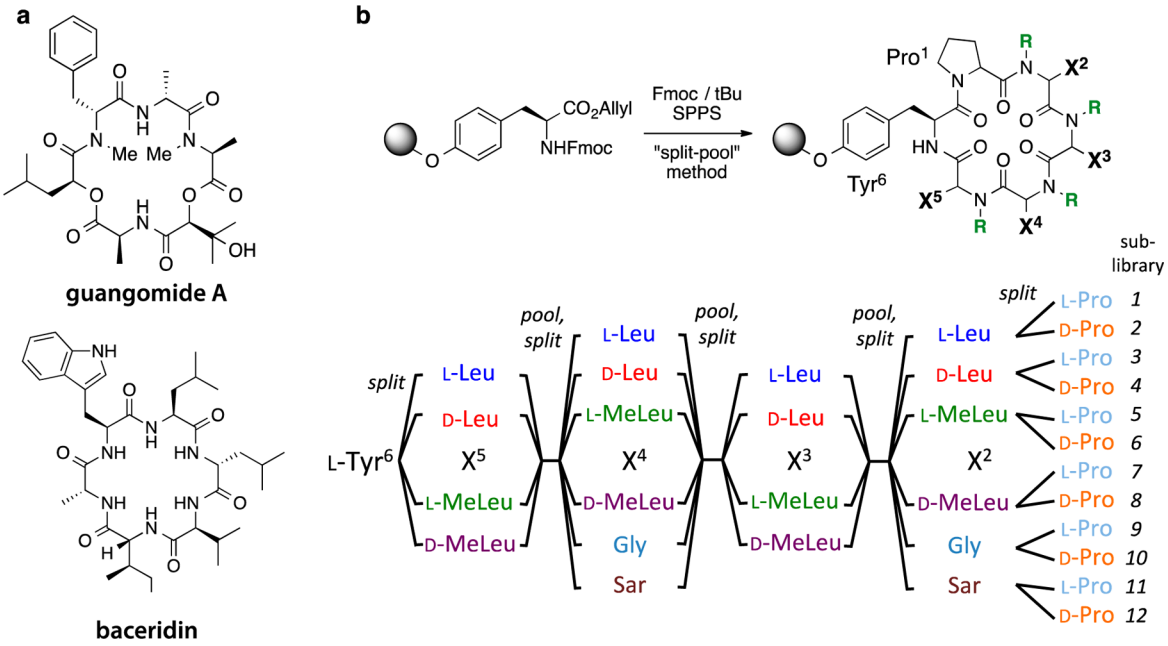

Figure 1. (a) Natural products similar to library members synthesized in this study. (b) Overall design of split-pool library of geometrically diverse cyclic hexapeptides.

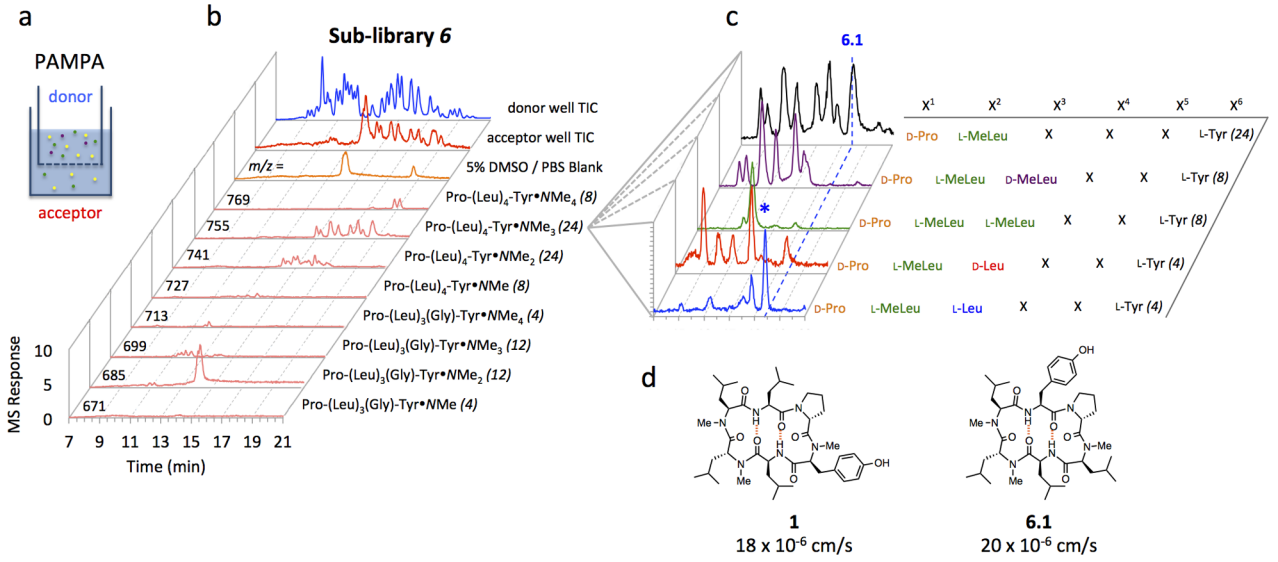

Figure 2. (a) Schematic of PAMPA in vitro permeability assay system. (b) LCMS traces from PAMPA analysis of sub-library *6*, showing extracted-ion chromatograms from acceptor well at *m*/*z* values corresponding to compositional variants. Included in italicized parentheses are the theoretical number of isomers contained in the corresponding donor wells for each mass. (c) Deconvolution of sub-library *6* by resynthesis of tier-2 sub-libraries in which X^3 is known. The major permeable component of the X^3 = L-Leu is shown with an asterisk and was identified as **6.1**, a sequence analogue of the previously identified (ref 23), highly permeable compound **1**. (d) Structures of **1** and **6.1**. Permeabilities shown below the structures were determined in Caco-2 cells.

guangomide A,[25] baceridin,[26] Figure 1a), and investigations into the relationship between conformation and permeability across small sets of structures present in the library. Our results confirm the importance of side-chain orientation and steric factors in determining membrane permeability in cyclic peptides, with implications for the design of synthetic, cell-permeable macrocycles.

RESULTS AND DISCUSSION

First, we designed a split-pool library[27] based on a cyclic hexapeptide template that would sample all possible stereoisomers and *N*-methyl variants, translating into diverse backbone geometries and conformational preferences. We employed the generic sequence Pro-$(Xaa)_4$-Tyr, incorporating L- and D-Leu, and L- and D-MeLeu at the variable positions X^2–X^5 (Figure 1b), and included Gly and MeGly (Sar) at positions X^2 and X^4 to investigate the impact of overall lipophilicity and backbone flexibility on permeability. Following library synthesis, LCMS showed that although expected impurities were observed, all expected masses were present in appropriate ratios predicted by the statistical representation of each isomeric series (see Supporting Information (SI)). The library design

DOI: 10.1021/ja508766b
J. Am. Chem. Soc. 2015, 137, 715–721

allowed unambiguous assignment of the composition (i.e., specifying the number of Leu vs Gly residues and the number of *N*-methyls) of each set of stereo- and constitutional isomers to an observed parent mass. Within each isomeric series there was good chromatographic separation of the individual compounds.

Passive membrane diffusion was quantified initially using the parallel artificial membrane permeability assay (PAMPA), an established cell-free membrane permeability system comprised of a donor and acceptor well separated by a filter impregnated with 1% lecithin in dodecane (Figure 2a).[28,29] After a period of incubation, compound flux across the dodecane layer was measured by LCMS analysis of the acceptor wells using selected ion monitoring (SIM), which allowed for the acquisition of mass-separated chromatogram traces (Figure 2b) corresponding to the different isomeric series. After synthesis and resin cleavage, we identified an average of ∼47 distinct peaks from each sub-library, or 567 peaks for the entire library. After PAMPA, ∼240 distinct peaks appeared in the acceptor wells. Although differences in the amounts of each species present in the donor wells precludes a quantitative assessment of the individual permeabilities at this stage in the analysis, nearly half of these peaks (∼105) showed significant intensity in their respective acceptor wells by rough MS quantitation (SI, Figure S4a). A significant portion of these peaks with high apparent permeability were concentrated in sub-libraries *4* and *6*. In general, sub-libraries with more *N*-methyl groups showed a greater overall enrichment in permeable compounds compared to sub-libraries with fewer *N*-methyls (Figure S4b), and sub-libraries with Gly or Sar residues were on average less permeable than the corresponding all-Leu-containing sub-libraries, with no permeable compounds detected containing two Gly/Sar residues (Figure S4c). There were exceptions to these trends; for example, some compounds with 4 *N*-Me groups showed very low permeability, while some non-*N*-methylated compounds appeared to be highly permeable (see below). Also, several Gly- and Sar-containing compounds showed strong enrichment in the PAMPA acceptor wells, suggesting that these scaffolds can adopt particularly permeable conformations that compensate for the decrease in lipophilicity resulting from the loss of a Leu side chain.

Next we set out to identify specific, membrane permeable scaffolds from the 12 sub-libraries, initially focusing on sub-library *6* with the consensus sequence cyclo[D-Pro^1–L-MeLeu^2–X^3–X^4–X^5–L-Tyr^6] (Figure 2c, top chromatogram). LCMS analysis of this sub-library showed a large number of permeable scaffolds in the m/z = 755 trace corresponding to cyclic peptides with three backbone *N*-methyl groups. Rather than synthesizing and testing all 24 tri-*N*-methylated stereochemical and *N*-methyl positional isomers in sub-library 6, we used a recursive deconvolution strategy[30] to identify selected peaks. Thus, four new "tier-2" sub-libraries with X^3 defined (as L-Leu, D-Leu, L-MeLeu, or D-MeLeu) (Figure 2c) were synthesized and submitted to PAMPA analysis. The resulting mixtures (simplified as expected compared to the parent sub-library) showed compounds with varying degrees of permeability, and follow-up studies on individual compounds led to scaffolds of known permeability, as well as novel scaffolds that revealed interesting structure–permeability relationships.

In the tier-2 sub-library in which X^3 = L-Leu (Figure 2c, blue chromatogram), the major permeable component was **6.1**, an analog that shares the same backbone scaffold as a compound (**1**) which we had identified previously using independent methods as a highly permeable and orally bioavailable scaffold (F = 28% in rat) (Figure 2d).[23] Compounds **6.1** and **1** share the same stereochemistry and *N*-methylation pattern, differing only in the side chains of the two amino acids on either side of the Pro. Indeed the low-dielectric conformation of **6.1** was predicted to be identical to the NMR solution conformation determined for **1** (SI, Figure S5).[23] The permeabilities of **6.1** and **1** were measured in the Caco-2 epithelial cell line and were found to be nearly identical (Figure 2d).

Most cyclic peptide natural products that are known to be cell permeable by passive diffusion contain at least one *N*-methylated backbone amide,[24] although synthetic cyclic hexapeptide scaffolds have been reported with no *N*-methyl groups that also show drug-like passive membrane permeability[21,22] and even oral bioavailability.[31] In the 1152-member library reported here, excluding compounds with glycine, there are 32 non-*N*-methylated cyclic peptides distributed exclusively among sub-libraries *1*–*4*. The combined extracted ion chromatograms from these sub-libraries showed 31 distinct peaks (at m/z = 713 corresponding to the non-*N*-methyl, non-Gly-containing isomers) in the PAMPA donor wells. At least 6 of these compounds showed significant enrichment in the PAMPA acceptor wells, with the most permeable species concentrated in sub-libraries *1* and *4*. In sub-library *4* (Figure 3a), 7 out of the 8 possible diastereomers were visible in the acceptor well chromatogram, with strong enrichment observed for two of the peaks (Figure 3b). All 8 isomers from sub-library *4* were synthesized individually and the identities of the peaks from the original mixture were confirmed by separate coinjections with each of the pure compounds.

Caco-2 permeability studies on the 8 non-*N*-methylated stereoisomers from sub-library *4* confirmed that the two most permeable isomers were **4.4** and **4.7** (Figure 3c, Table 1). The predicted backbone conformations of both **4.4** and **4.7** are near mirror images of the NMR-derived solution conformation of compound **2**, which we had previously identified as having drug-like passive permeability by PAMPA.[22] At the backbone level, **4.7** and **2** are indeed enantiomers, and **4.4** differs from **4.7** by a single stereocenter (position X^3). Moreover, among the least permeable isomers in the series was **4.3** (Figure 3d, Table 1) in which both the X^4 and X^5 stereocenters are inverted with respect to compounds **4.4** and **4.7**. The predicted conformation for **4.3** was nearly identical to the NMR solution structure in $CDCl_3$ of **3**, revealing the highly exposed amide NH that is most likely responsible for the poor permeability of both compounds. Variable temperature ^{1}H NMR (VT-NMR), which has been used as a tool to provide evidence of hydrogen bonding or solvent exclusion within proteins,[32,33] supports these interpretations (SI, Table S10). The small temperature shift coefficients (<4 ppb/K) of all NH groups in **4.4** and **4.7** are consistent their relatively high cell permeabilities, and also with the prediction, based on computational studies and their structural similarity to compound **2**, that all amides in these compounds are protected from solvent (either through intramolecular hydrogen bonding or, in the case of L-Leu^4, by steric occlusion).[22] On the other hand, two of the temperature shift coefficients in **4.3** are greater than 4 ppb/K, consistent with the two solvent-exposed amides found in the solution NMR structure (in $CDCl_3$) of its congener **3**, and also consistent with the relatively low cell permeabilities of both **3** and **4.3**. Thus, this screening/deconvolution approach not only independently identified the enantiomer of a scaffold known to

DOI: 10.1021/ja508766b
J. Am. Chem. Soc. 2015, 137, 715–721

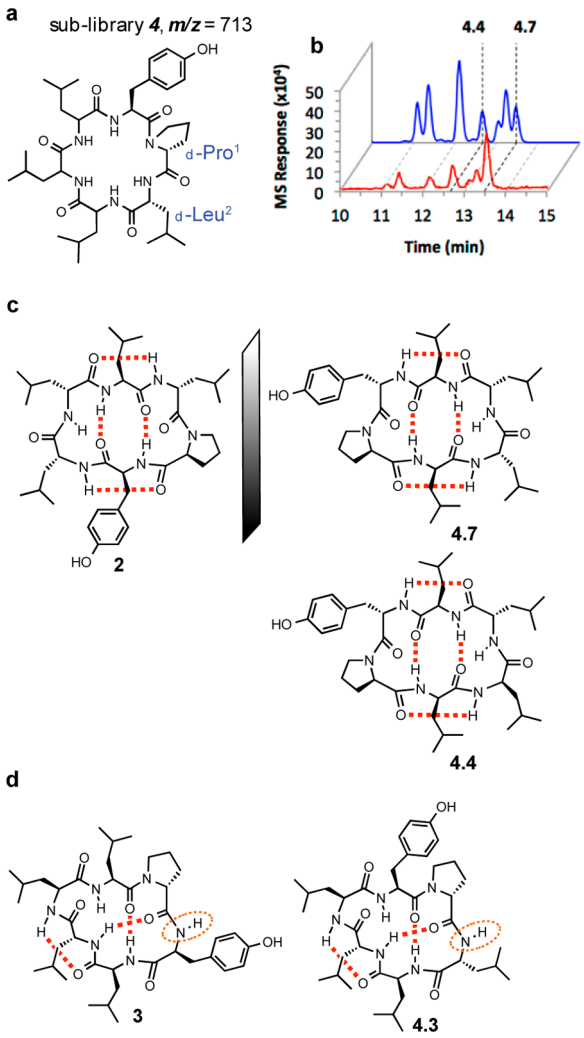

Figure 3. (a) General structure of sub-library *4* at m/z = 713, corresponding to non-*N*-methylated scaffolds. (b) HPLC traces of chromatogram (extracted ion monitoring at m/z = 713) for donor (blue) and acceptor (red) wells following PAMPA analysis of sub-library *4*. (c) Structures of compound **2** from an earlier study (ref 22) and two pseudoenantiomers from this study, **4.4** and **4.7**. (d) Structures of compound **3** from the same previous study and analogue **4.3**, highlighting their most solvent-exposed NH group.

Table 1. Sequence and Measured Permeation Rates for Non-*N*-methylated Compounds from Sub-library 4

compd	t_R (min)	X^3	X^4	X^5	P_e ($\times 10^{-6}$ cm/s)[a]
4.1	11.1	D-Leu	L-Leu	L-Leu	0.26
4.2	11.3	L-Leu	L-Leu	L-Leu	0.43
4.3	12.1	L-Leu	D-Leu	L-Leu	0.14
4.4	12.7	D-Leu	L-Leu	D-Leu	7.9
4.5	13.1	D-Leu	D-Leu	D-Leu	0.045
4.6	13.2	L-Leu	D-Leu	D-Leu	0.5
4.7	13.5	L-Leu	L-Leu	D-Leu	3.6
4.8	nd	D-Leu	D-Leu	L-Leu	0.23

[a]As measured by Caco-2 assay.

have good membrane permeability, but it also suggests that the stereocenter at Leu[3] can be inverted without changing the backbone conformation or compromising permeability.

In both series of compounds discussed thus far, the tri-*N*-methylated scaffold of **6.1** and the non-*N*-methylated scaffolds of **4.4** and **4.7**, the major conformation-defining features are the overlapping β-turns that enforce two strong, transannular hydrogen bonds. In **6.1**, the other three solvent-exposed amide NH groups are *N*-methylated, whereas in **4.4**, two of the solvent-exposed amides are forced into extra-annular γ-turns, creating a bowl-shaped structure that orients the remaining free NH into the center of the bowl and away from solvent. Upon further deconvolution of the tri-*N*-methylated compounds from sub-library *6*, we were intrigued to find that among the most permeable compounds in one of the tier-2 sub-libraries were compounds corresponding to the consensus sequence cyclo[D-Pro[1]–L-MeLeu[2]–D-MeLeu[3]–D/L-MeLeu[4]–D/L-Leu[5]–L-Tyr[6]] (Figure 2c, purple chromatogram), in which the two non-*N*-methylated residues were contiguous (Figure 4a). Since this arrangement of *N*-Me and NH groups would appear to preclude the type of β-turn architecture found in **4.4**, **4.7**, and **6.1**, we set out to investigate this scaffold further by synthesizing and testing all eight permutations within the X^3 = D-MeLeu tier-2 sub-library. The two most cell permeable compounds in this series, **6.7** and **6.9**, differed only in the configuration at MeLeu[4], while the most- and least-permeable compounds, **6.7** and **6.6**, also differed by a single stereocenter at Leu[5] despite a 60-fold difference in Caco-2 permeabilities (Figure 4a).

We used a combination of computational and NMR approaches to investigate the underlying structural/conformational basis for the large variation in permeability among the closely related stereoisomeric series **6.6**–**6.9**. First, 2D ROESY NMR experiments (in the low dielectric solvent $CDCl_3$) of **6.9**, one of the two most permeable compounds in the series, revealed that the two contiguous, non-*N*-methylated residues enforce two overlapping, somewhat distorted γ-turns (Figure 4b). Because of this distortion, neither of the amide NH groups in **6.9** are involved in a classic hydrogen bond.[34,35] The computationally predicted conformation of **6.9** was also consistent with its NMR structure, with a backbone RMSD of 0.27 Å between the two structures (SI, Figure S3c). Indeed, while the four stereoisomers **6.6**–**6.9** were predicted to adopt very similar backbone conformations (average RMSD = 0.5 Å), intramolecular hydrogen bonds were observed in only two of the compounds, **6.6** and **6.8** (as γ-turns between MeLeu[4] and Leu[5]). Paradoxically, **6.6** and **6.8** are the two least permeable compounds in the series, while neither of the most permeable compounds, **6.7** and **6.9**, showed any intramolecular hydrogen bonding. Nonetheless, in all four isomers, both NH groups point well into the interior of the macrocycle, shielding all of the amides from solvent, including those not involved in hydrogen bonds.

The cell permeabilities in **6.6**–**6.9** are most influenced by the configuration at Leu[5]: in **6.7** and **6.9**, the D-Leu[5] side chains project over the macrocycle center, while the L-Leu[5] side chains of **6.6** and **6.8** project away from the ring (Figure 4b). In contrast, permeabilities are much less sensitive to the configuration at MeLeu[4], where the side chains orient away from the macrocycle, irrespective of stereochemistry at that position. The different side-chain orientations give rise to different calculated 3D solvent accessible surface areas (SASA), as the projection of the Leu[5] side chains in **6.7** and **6.9** over one face of the macrocycle partially shield its polar interior from solvent (Figure 4c). This variation in 3D SASA (101.6 and 104.5 Å for **6.7** and **6.9**, vs 140.5 and 125.7 Å for **6.8** and **6.6**, respectively) in turn gives rise to corresponding differences in calculated desolvation energies (ΔG_{desolv}), and indeed both 3D

DOI: 10.1021/ja508766b
J. Am. Chem. Soc. 2015, 137, 715–721

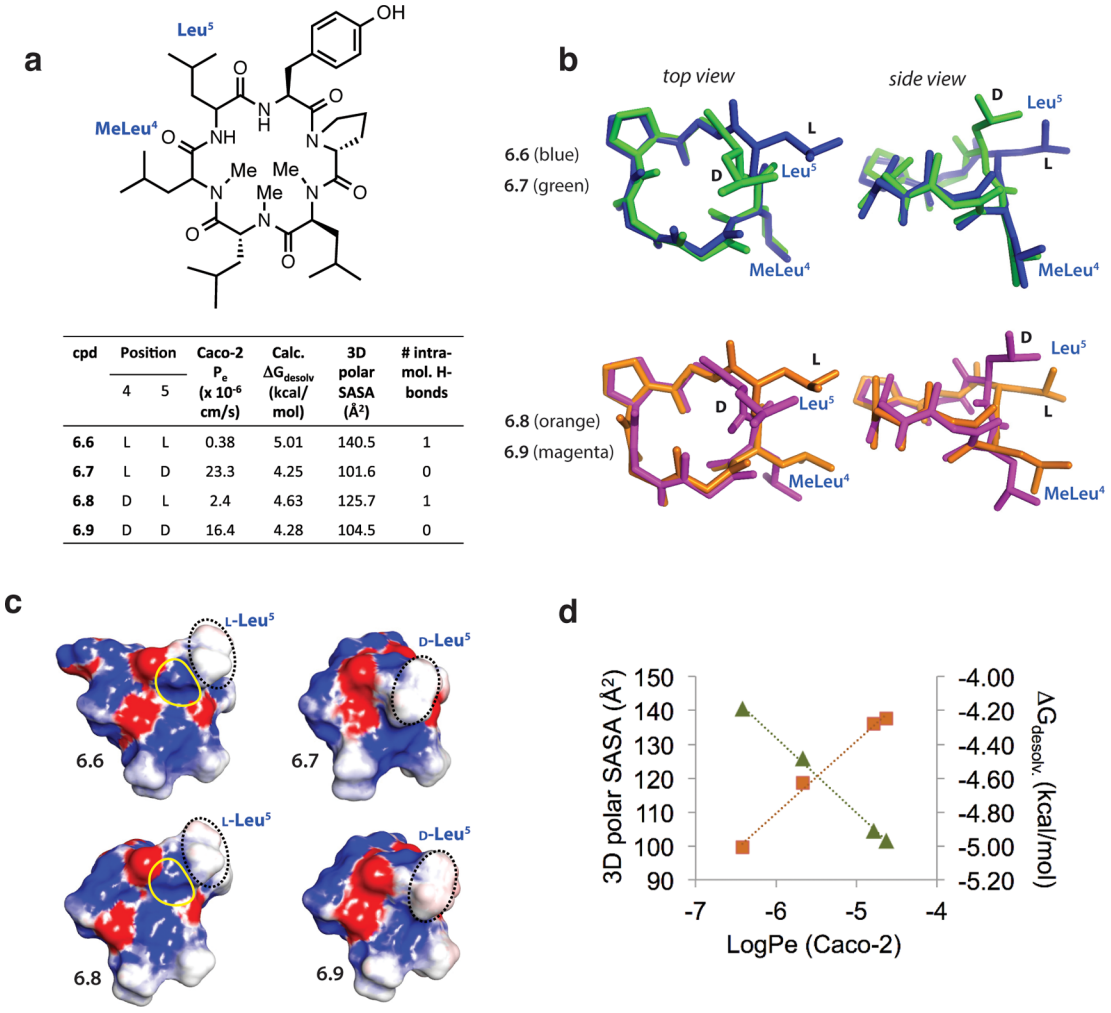

cpd	Position 4	Position 5	Caco-2 P_e (x 10^{-6} cm/s)	Calc. ΔG_{desolv} (kcal/mol)	3D polar SASA (Å^2)	# intramol. H-bonds
6.6	L	L	0.38	5.01	140.5	1
6.7	L	D	23.3	4.25	101.6	0
6.8	D	L	2.4	4.63	125.7	1
6.9	D	D	16.4	4.28	104.5	0

Figure 4. (a) General structure of compounds **6.6**–**6.9**, their Caco-2 permeabilities, predicted desolvation energies and 3D polar solvent accessible surface areas (SASA), and number of intramolecular hydrogen bonds. (b) Top and side views of compounds **6.6** (blue), **6.7** (green), **6.8** (orange), and **6.9** (magenta) overlaid (for clarity, only the side chains of residues MeLeu^4 and Leu^5 are shown). (c) Electrostatic surfaces (red = $\delta-$, blue = $\delta+$, white = neutral) of predicted low-dielectric conformers of **6.6**–**6.9**, with the orientation of the Leu^5 side chains highlighted in gray dashed ovals. Outlined in yellow is the portion of the polar surface in **6.6** and **6.8** that is effectively masked by the D-Leu^5 side chains in **6.7** and **6.9**. (d) Plot of predicted desolvation energy (orange) and 3D polar SASA (green) vs Caco-2 permeabilities of the four compounds.

SASA and ΔG_{desolv} are highly correlated with Caco-2 permeabilities in this set (Figure 4d). These results highlight the existence of "permeability cliffs" among closely related cyclic peptide scaffolds that differ only by relative stereochemistry, and also demonstrate that steric occlusion of polar groups from solvent can outweigh intramolecular hydrogen bonding in the relationship between structure and permeability in cyclic peptides.

Having discovered several cyclic peptides with measurable membrane permeability, we wanted to investigate whether one of these scaffolds could be diversified at the side-chain level while retaining favorable membrane permeability. Therefore, we used our split-pool approach to generate side-chain variants based on the permeable scaffold **4.7** and tested their permeabilities by PAMPA, including the parent scaffold as an internal control. Three new libraries were synthesized in which positions 3, 4, and 5 were varied among amino acids with a variety of side-chain functionalities, including a basic residue (Orn), a hydrogen bond donor (Thr) and acceptor (4-Pal), and various nonpolar residues of natural and non-natural origin (Ala, Abu, Val, Phe, 2-Nal, and Cha) (SI, Figure S6). In general, substitutions that led to a decrease in lipophilicity were detrimental to permeability, while those that retained or increased lipophilicity showed similar or improved permeability compared to the parent **4.7** (Figure 5). For the highly lipophilic substitution Nal, the variability in PAMPA values could be attributable to the low recovery, most likely due to solubility or aggregation issues. The permeability trends among the side-chain variants were the same for each substituted position. These results suggest that diverse libraries generated from side-chain variants of permeable scaffolds such as **4.7** (e.g., for use as input into biochemical screens) can maintain the permeability of the parent scaffold at least within a reasonable lipophilicity window.[37]

CONCLUSIONS

We have described a combinatorial library/deconvolution approach to the discovery of cell permeable cyclic peptide scaffolds. The methodology reported here, based on the synthesis and direct permeability analysis of complex cyclic peptide mixtures, was validated by the discovery of analogues of two cyclic peptides known to be passively permeable and, in

DOI: 10.1021/ja508766b
J. Am. Chem. Soc. 2015, 137, 715–721

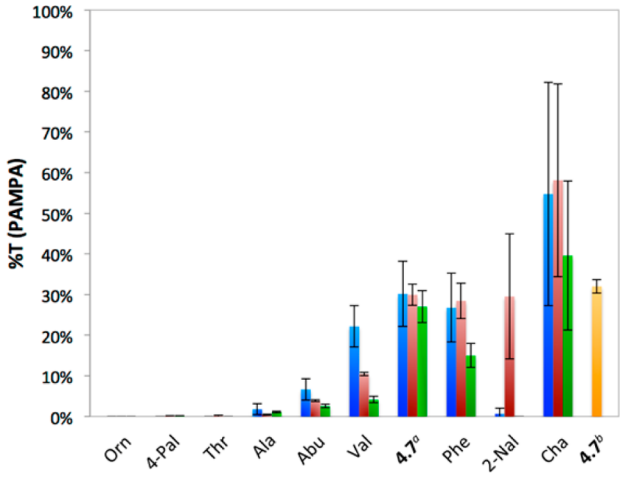

Figure 5. PAMPA permeability of Leu[3]Xaa (blue), Leu[4]Xaa (red), and Leu[5]Xaa (green) diversified analogues of compound **4.7** within split-pool single-point diversity libraries. [Notes: [a]Refers to compound **4.7** synthesized within each library. [b]Refers to the permeability of **4.7** as an external reference.

one case, orally bioavailable. We have also found, consistent with studies in other systems,[31,36] that subtle factors such as side-chain orientation can significantly impact permeability by sterically masking polar backbone atoms. Indeed, in our earlier studies on **2** and **3**, we found that the steric occlusion of backbone amides could be as effective as internal hydrogen bonding in increasing permeability,[22] which was corroborated by later computational studies demonstrating that intramolecular hydrogen bond counts are not as predictive of permeability as more quantitative descriptors such as 3D polar SASA.[21] Furthermore, while this manuscript was under review, a paper published by Nielsen, et al., showed the same phenomenon in synthetic analogs of the cyclic peptide natural product sanguinamide A, in which steric occlusion of polar groups by bulky side chains led to improved oral bioavailability.[38] These results, along with ours demonstrating the shielding effect of stereochemistry on permeability, raise the question as to whether steric factors related to side-chain positioning are also at play in the extraordinary permeability of other cyclic peptide natural products such as CSA.

This study also demonstrates the power of using a library/deconvolution approach to identify permeable scaffolds from complex mixtures, as validated by the independent scaled-up resynthesis and characterization of several compounds identified as hits in the initial screen. The power of this approach lies in the ability to separate compounds of interest from complex mixtures by selected ion monitoring-LCMS, and to determine permeabilities by comparison between input and output chromatogram traces. The observation that upon deconvolution the simplified sub-libraries are enriched in permeable species, adds further confidence in the utility of the initial libraries despite their high complexity.

It may be useful to put the approach to scaffold discovery reported here in the context of the large DNA-encoded libraries and display technologies[39] that have emerged over the past few decades. Very large and diverse cyclic peptide libraries have been generated using these approaches; however, since these library designs rarely take cell permeability into account, few of the resulting lead compounds are permeable despite some impressive biochemical potencies.[40,41] The scaffolds reported herein (including many that have yet to be fully deconvoluted) may provide a means to bias the design of DNA-encoded libraries toward cell permeability from the outset, for example, by varying side chains on scaffolds with high intrinsic permeability. Such designs would also benefit from a deeper understanding of the relationship between overall side-chain lipophilicity and permeability, so that chemical properties can be optimized for permeability while maintaining a high degree of both chemical and geometric diversity.

Here we have shown that relatively complex and conformationally diverse cyclic peptides can be achieved with simple building blocks and chemistries that are compatible (for the most part) with DNA-encoded libraries and other diversity approaches, suggesting a path toward larger libraries biased toward cell permeability. Our finding that the cell permeability of a particular scaffold can be maintained upon side-chain substitution provides further optimism that such a bias can be achieved, provided that side chains are selected to maintain an appropriate level of lipophilicity. Variations on scaffold **4.7**, which is not *N*-methylated and has only a moderate Caco-2 permeability, suggest that any decrease in lipophilicity is detrimental to permeability in this scaffold. We predict that the same substitutions performed on more intrinsically permeable, *N*-methylated scaffolds such as **6.7**, will show a wider "lipophilicity window" within which permeability can be achieved. Work is now underway to further deconvolute the permeable species in the library reported here, and to quantify in more detail the impact of side-chain lipophilicity on permeability in the context of other scaffolds.

■ ASSOCIATED CONTENT

Supporting Information

Experimental details for the synthesis of individual cyclic peptides and cyclic peptide sub-libraries, details for PAMPA analysis of cyclic peptide sub-libraries and Caco-2 assay of pure cyclic peptides, LCMS chromatograms and direct inject mass spectra for sub-libraries, LCMS chromatograms and ^{1}HNMR spectra for individual cyclic peptides, details for computational structure generation, 2D NMR spectra for **6.9** and details for solution structure generation, and measured permeation rates via Caco-2 assay for all individually synthesized cyclic peptides and controls. This material is available free of charge via the Internet at http://pubs.acs.org.

■ AUTHOR INFORMATION

Corresponding Authors

matt.jacobson@ucsf.edu
slokey@ucsc.edu

Present Address

[⊥]S.S.F.L.: Circle Pharma, Inc., San Francisco, CA 94107

Notes

The authors declare the following competing financial interest(s): M.P.J. is a consultant to Pfizer and Schrodinger LLC, and co-founder of Circle Pharma. R.S.L. is a cofounder of Circle Pharma.

■ ACKNOWLEDGMENTS

This work was funded by a research grant from MedImmune, Ltd.

DOI: 10.1021/ja508766b
J. Am. Chem. Soc. 2015, 137, 715−721

REFERENCES

(1) Overington, J. P.; Al-Lazikani, B.; Hopkins, A. L. *Nat. Rev. Drug Discov.* **2006**, *5*, 993.
(2) Malovannaya, A.; Lanz, R. B.; Jung, S. Y.; Bulynko, Y.; Le, N. T.; Chan, D. W.; Ding, C.; Shi, Y.; Yucer, N.; Krenciute, G.; Kim, B. J.; Li, C.; Chen, R.; Li, W.; Wang, Y.; O'Malley, B. W.; Qin, J. *Cell* **2011**, *145*, 787.
(3) Colby, D. W.; Chu, Y.; Cassady, J. P.; Duennwald, M.; Zazulak, H.; Webster, J. M.; Messer, A.; Lindquist, S.; Ingram, V. M.; Wittrup, K. D. *Proc. Natl. Acad. Sci. U.S.A.* **2004**, *101*, 17616.
(4) Kenne, E.; Renne, T. *Drug Discov. Today* **2014**, *9*, 1459.
(5) Reichert, J. M.; Dhimolea, E. *Drug Discov. Today* **2012**, *17*, 954.
(6) Passioura, T.; Katoh, T.; Goto, Y.; Suga, H. *Annu. Rev. Biochem.* **2014**, *83*, 727.
(7) Kawamoto, S. A.; Coleska, A.; Ran, X.; Yi, H.; Yang, C. Y.; Wang, S. *J. Med. Chem.* **2012**, *55*, 1137.
(8) Madden, M. M.; Muppidi, A.; Li, Z.; Li, X.; Chen, J.; Lin, Q. *Bioorg. Med. Chem. Lett.* **2011**, *21*, 1472.
(9) Moellering, R. E.; Cornejo, M.; Davis, T. N.; Del Bianco, C.; Aster, J. C.; Blacklow, S. C.; Kung, A. L.; Gilliland, D. G.; Verdine, G. L.; Bradner, J. E. *Nature* **2009**, *462*, 182.
(10) Liu, T.; Joo, S. H.; Voorhees, J. L.; Brooks, C. L.; Pei, D. *Bioorg. Med. Chem.* **2009**, *17*, 1026.
(11) Gavenonis, J.; Sheneman, B. A.; Siegert, T. R.; Eshelman, M. R.; Kritzer, J. A. *Nat. Chem. Biol.* **2014**, *10*, 716.
(12) Passioura, T.; Suga, H. *Chemistry* **2013**, *19*, 6530.
(13) Quartararo, J. S.; Wu, P.; Kritzer, J. A. *ChemBioChem* **2012**, *13*, 1490.
(14) Wrighton, N. C.; Farrell, F. X.; Chang, R.; Kashyap, A. K.; Barbone, F. P.; Mulcahy, L. S.; Johnson, D. L.; Barrett, R. W.; Jolliffe, L. K.; Dower, W. J. *Science* **1996**, *273*, 458.
(15) Lipinski, C.; Lombardo, F.; Dominy, B.; Feeney, P. *Adv. Drug Delivery Rev.* **1997**, *23*, 3.
(16) Lipinski, C. A. *J. Pharmacol. Toxicol. Methods* **2000**, *44*, 235.
(17) Swift, R. V.; Amaro, R. E. *Chem. Biol. Drug Des.* **2013**, *81*, 61.
(18) Guimaraes, C. R.; Mathiowetz, A. M.; Shalaeva, M.; Goetz, G.; Liras, S. *J. Chem. Inf. Model.* **2012**, *52*, 882.
(19) Kotz, J. *SciBX* **2012**, *5*, 1.
(20) Villar, E. A.; Beglov, D.; Chennamadhavuni, S.; Porco, J. A., Jr.; Kozakov, D.; Vajda, S.; Whitty, A. *Nat. Chem. Biol.* **2014**, *10*, 723.
(21) Rezai, T.; Bock, J.; Zhou, M.; Kalyanaraman, C.; Lokey, R.; Jacobson, M. *J. Am. Chem. Soc.* **2006**, *128*, 14073.
(22) Rezai, T.; Yu, B.; Millhauser, G.; Jacobson, M.; Lokey, R. *J. Am. Chem. Soc.* **2006**, *128*, 2510.
(23) White, T. R.; Renzelman, C. M.; Rand, A. C.; Rezai, T.; McEwen, C. M.; Gelev, V. M.; Turner, R. A.; Linington, R. G.; Leung, S. S.; Kalgutkar, A. S.; Bauman, J. N.; Zhang, Y.; Liras, S.; Price, D. A.; Mathiowetz, A. M.; Jacobson, M. P.; Lokey, R. S. *Nat. Chem. Biol.* **2011**, *7*, 810.
(24) Bockus, A. T.; McEwen, C. M.; Lokey, R. S. *Curr. Top. Med. Chem.* **2013**, *13*, 821.
(25) Amagata, T.; Morinaka, B. I.; Amagata, A.; Tenney, K.; Valeriote, F. A.; Lobkovsky, E.; Clardy, J.; Crews, P. *J. Nat. Prod.* **2006**, *69*, 1560.
(26) Niggemann, J.; Bozko, P.; Bruns, N.; Wodtke, A.; Gieseler, M. T.; Thomas, K.; Jahns, C.; Nimtz, M.; Reupke, I.; Bruser, T.; Auling, G.; Malek, N.; Kalesse, M. *ChemBioChem* **2014**, *15*, 1021.
(27) Lam, K. S.; Salmon, S. E.; Hersh, E. M.; Hruby, V. J.; Kazmierski, W. M.; Knapp, R. J. *Nature (London, United Kingdom)* **1991**, *354*, 82.
(28) Avdeef, A.; Bendels, S.; Di, L.; Faller, B.; Kansy, M.; Sugano, K.; Yamauchi, Y. *J. Pharm. Sci.* **2007**, *96*, 2893.
(29) Kansy, M.; Senner, F.; Gubernator, K. *J. Med. Chem.* **1998**, *41*, 1007.
(30) Erb, E.; Janda, K. D.; Brenner, S. *Proc. Natl. Acad. Sci. U.S.A.* **1994**, *91*, 11422.
(31) Hill, T. A.; Lohman, R.-J.; Hoang, H. N.; Nielsen, D. S.; Scully, C. C. G.; Kok, W. M.; Liu, L.; Lucke, A. J.; Stoermer, M. J.; Schroeder, C. I.; Chaousis, S.; Colless, B.; Bernhardt, P. V.; Edmonds, D. J.; Griffith, D. A.; Rotter, C. J.; Ruggeri, R. B.; Price, D. A.; Liras, S.; Craik, D. J.; Fairlie, D. P. *ACS Med. Chem. Lett.* **2014**, *10*, 1148.
(32) Hong, J.; Jing, Q.; Yao, L. *J. Biomol. NMR* **2013**, *55*, 71.
(33) Cordier, F.; Grzesiek, S. *J. Mol. Biol.* **2002**, *317*, 739.
(34) Baker, E. N.; Hubbard, R. E. *Prog. Biophys. Mol. Biol.* **1984**, *44*, 97.
(35) Bissantz, C.; Kuhn, B.; Stahl, M. *J. Med. Chem.* **2010**, *53*, 5061.
(36) Nielsen, D. S.; Hoang, H. N.; Lohman, R. J.; Diness, F.; Fairlie, D. P. *Org. Lett.* **2012**, *14*, 5720.
(37) Waring, M. J. *Bioorg. Med. Chem. Lett.* **2009**, *19*, 2844.
(38) Nielsen, D. S.; Hoang, H. N.; Lohman, R. J.; Hill, T. A.; Lucke, A. J.; Craik, D. J.; Edmonds, D. J.; Griffith, D. A.; Rotter, C. J.; Ruggeri, R. B.; Price, D. A.; Liras, S.; Fairlie, D. P. *Angew. Chem., Int. Ed.* **2014**, *53*, 12059.
(39) Franzini, R. M.; Neri, D.; Scheuermann, J. *Acc. Chem. Res.* **2014**, *47*, 1247−1255.
(40) Georghiou, G.; Kleiner, R. E.; Pulkoski-Gross, M.; Liu, D. R.; Seeliger, M. A. *Nat. Chem. Biol.* **2012**, *8*, 366−374.
(41) Yamagishi, Y.; Shoji, I.; Miyagawa, S.; Kawakami, T.; Katoh, T.; Goto, Y.; Suga, H. *Chem. Biol.* **2011**, *18*, 1562−1570.

NOTE ADDED AFTER ASAP PUBLICATION

This paper was published on January 8, 2015 with errors in the compound numbering in the third to last paragraph in the Results and Discussion section. This has been corrected and the paper was re-posted on January 12, 2015.

DOI: 10.1021/ja508766b
J. Am. Chem. Soc. 2015, 137, 715−721